Molecular Therapy
Methods & Clinical Development
Original Article

Testing the efficacy of a human full-length OPG-Fc analog in a severe model of cardiotoxin-induced skeletal muscle injury and repair

Zineb Bouredji,[1] Dounia Hamoudi,[1] Laetitia Marcadet,[1] Anteneh Argaw,[1] and Jérôme Frenette[1,2]

[1]Centre Hospitalier Universitaire de Québec, Centre de Recherche du Centre Hospitalier de l'Université Laval (CHUQ-CHUL), Axe Neurosciences, Université Laval, Quebec City, QC G1V 4G2, Canada; [2]Département de Réadaptation, Faculté de Médecine, Université Laval, Quebec City, QC G1V 0A6, Canada

Although receptor-activator of nuclear factor κB (RANK), its ligand RANKL, and osteoprotegerin (OPG), which are members of the tumor necrosis factor (TNF) superfamily, were first discovered in bone cells, they are also expressed in other cells, including skeletal muscle. We previously showed that the RANK/RANKL/OPG pathway is involved in the physiopathology of Duchenne muscular dystrophy and that a mouse full-length OPG-Fc (mFL-OPG-Fc) treatment is superior to muscle-specific RANK deletion in protecting dystrophic muscles. Although mFL-OPG-Fc has a beneficial effect in the context of muscular dystrophy, the function of human FL-OPG-Fc (hFL-OPG-Fc) during muscle repair is not yet known. In the present study, we investigated the impacts of an hFL-OPG-Fc treatment following the intramuscular injection of cardiotoxin (CTX). We show that a 7-day hFL-OPG-Fc treatment improved force production of soleus muscle. hFL-OPG-Fc also improved soleus muscle integrity and regeneration by increasing satellite cell density and fiber cross-sectional area, attenuating neutrophil inflammatory cell infiltration at 3 and 7 days post-CTX injury, increasing the anti-inflammatory M2 macrophages 7 days post-CTX injury. hFL-OPG-Fc treatment also favored M2 over M1 macrophage phenotypic polarization *in vitro*. We show for the first time that hFL-OPG-Fc improved myotube maturation and fusion *in vitro* and reduced cytotoxicity and cell apoptosis. These findings demonstrate that hFL-OPG-Fc has therapeutic potential for muscle diseases in which repair and regeneration are impaired.

INTRODUCTION

Receptor-activator of nuclear factor κB (RANK), its ligand RANKL, and osteoprotegerin (OPG) are members of the tumor necrosis factor (TNF) superfamily and constitute the most important signaling pathway in bone homeostasis.[1] OPG is a soluble decoy receptor secreted by osteoblasts that neutralizes RANKL and prevents the osteoporotic process.[2] Although well characterized in bone, RANK, RANKL, and OPG are also expressed in other tissues, including smooth muscle, heart muscle, and skeletal muscle, but their roles in these tissues are not clearly defined.[3–5] In skeletal muscle, they have been associated with the modulation of inflammation and regeneration following eccentric muscle damage.[6] More recently, it was shown that OPG secreted by type II fast-twitch myofibers exerts an anti-inflammatory effect and protects pancreatic β cells against TNF-α-induced insulin resistance.[7] Alternatively, mice lacking OPG exhibit muscle weakness and selective muscle atrophy of fast-twitch myofibers,[8] which provides additional support for the notion that OPG plays a protective role in bone and muscle homeostasis and that a dysregulation in the RANKL/OPG ratio in the vicinity of muscle cells may potentially lead to muscular dysfunctions/diseases.

Resident inflammatory cells as well as recruited neutrophils and macrophages can release pro-inflammatory cytokines as part of a highly orchestrated myogenic and satellite cell activation process to ensure muscle repair.[9] Following injury, neutrophils are recruited and play an important role in phagocytosis of cellular debris, and in releasing chemokines, oxidative factors, and enzymes, enabling the recruitment of monocytes.[10,11] However, a massive and uncontrolled recruitment of neutrophils has also been associated with the induction of collateral damage following ischemia-reperfusion of muscle tissue.[12] Alternatively, monocytes, once recruited, rapidly differentiate into pro-inflammatory M1 macrophages ($F4/80^+/CD206^-$) soon after infiltration into injured tissues.[13,14] M1 macrophages switch their phenotype to anti-inflammatory M2 macrophages ($F4/80^+/CD206^+$) during the resolution of the inflammatory reaction, supporting myogenesis and myofiber growth and expressing very high levels of anti-inflammatory cytokines and growth factors.[14,15] Therefore, a controlled and timely inflammatory process is crucial for triggering the muscle repair and healing process with limited scar tissues. We have shown that a 10-day treatment with mouse full-length OPG fused to an Fc fragment (mFL-OPG-Fc) improves muscle function in a dystrophin-deficient mdx mouse, a rodent model for Duchenne muscular dystrophy (DMD).[5,16] RANK/RANKL protein levels are higher in the microenvironment of dystrophic

Received 4 May 2020; accepted 25 March 2021;
https://doi.org/10.1016/j.omtm.2021.03.022.

Correspondence: Jérôme Frenette, Centre Hospitalier Universitaire de Québec, Centre de Recherche du Centre Hospitalier de l'Université Laval (CHUQ-CHUL), Axe Neurosciences, Université Laval, Quebec City, QC G1V 4G2, Canada.
E-mail: jerome.frenette@crchudequebec.ulaval.ca

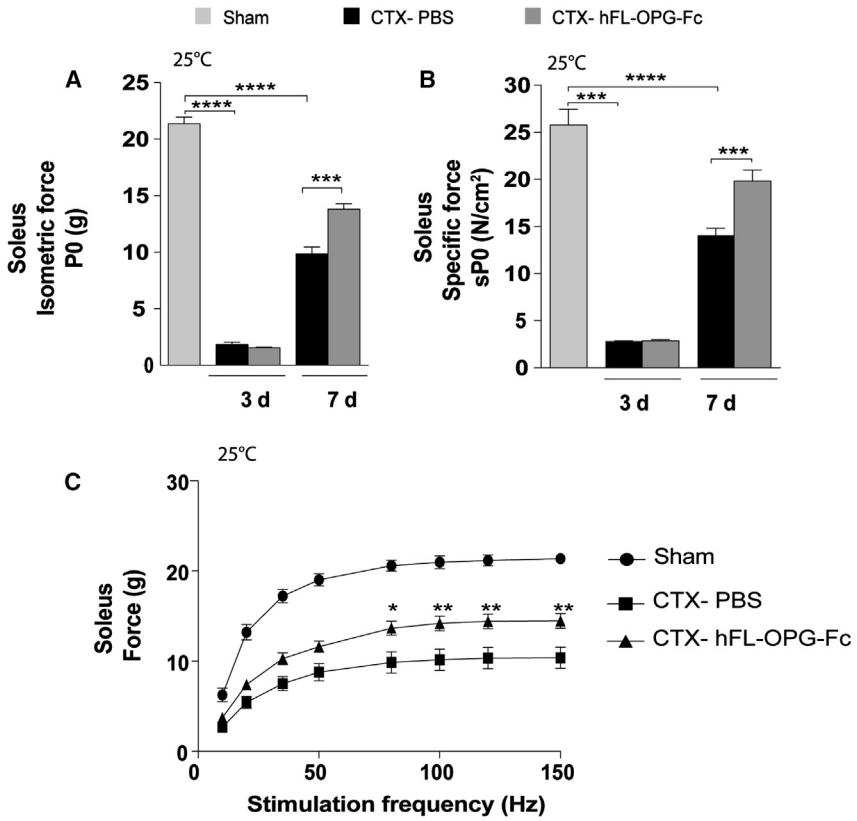

Figure 1. An hFL-OPG-Fc treatment significantly improved injured soleus (Sol) muscle function

The slow-twitch Sol muscles from 12-week-old-C57BL/10J mice were injected with 15 μL of cardiotoxin (CTX; 20 μM). The mice were then treated daily with either vehicle (PBS) or hFL-OPG-Fc (1 mg/kg/day) for 3 (n = 3) or 7 days (n = 7–12). The contractile properties were evaluated *ex vivo*. (A and B) Although untreated and treated mice presented a similar loss of force at day 3, injured Sol muscles from hFL-OPG-Fc-treated mice exhibited a significant improvement in isometric (P_0; A) and specific forces (sP_0; B) compared to PBS-treated mice at day 7. (C) The force frequency curve of Sol muscles from hFL-OPG-Fc-treated mice at day 7 exhibited a marked increase in force production compared to Sol muscles from PBS-treated mice. The muscle mass and twitch force (Pt) of Sol muscles from CTX-treated mice were significantly lower than those of Sol muscles from sham mice at 7 days post-injury. No other morphological or contractile parameters were significantly different (Table 1). Data are expressed as means ± SEM. *p < 0.05, **p < 0.01, and ***p < 0.001 indicate significantly different from PBS-treated mice, and ****p < 0.0001 designates significantly different from sham using an analysis of variance with Dunnett's test (one-way ANOVA) for multiple comparisons.

muscles.[17] The inhibition of their interaction with anti-RANKL antibody results in less muscle damage, fibrosis, edema, and inflammation.[17] Blockage of RANKL/RANK interaction also inhibits the NF-κB pathway, thereby regulating inflammation and the proportion of anti-inflammatory and non-cytotoxic M2 macrophages.[17] Interestingly, mFL-OPG-Fc is more effective in preserving dystrophic muscle function than muscle-specific *Rank* deletion or truncated OPG (TR-OPG-Fc; with only the RANKL binding domains),[16] suggesting that mFL-OPG-Fc may potentially impact different cellular processes in various tissues. Structurally, the FL-OPG-Fc protein contains four TNF receptor (TNFR)-like domains (RANKL binding sites), two death domains (TNF-related apoptosis-inducing ligand [TRAIL] binding sites), and a highly basic heparin-binding domain.[18] OPG promotes cell survival through its TRAIL-binding domains and cell proliferation, and migration through its highly basic heparin-binding domain in vascular, immune, and tumor cells,[19–21] in addition to its implication in human peripheral blood monocyte chemiotaxis.[22] Although mFL-OPG-Fc has a beneficial effect on dystrophic muscles, it cannot be translated into clinical applications. Mouse and human OPG amino acid sequence alignment shows that 85% of the amino acids are identical while 6% are similar and 9% are different (https://www.uniprot.org/; see also Figure S1). We thus investigated the beneficial effects of human FL-OPG-Fc (hFL-OPG-Fc) in a well-established and controlled model of cardiotoxin (CTX)-induced muscle injury and repair *in vitro* and *in vivo*.

In the present study, we show that a 7-day hFL-OPG-Fc treatment improved muscle force following CTX-induced injury. Furthermore, the hFL-OPG-Fc treatment attenuated CTX-induced neutrophil infiltration at days 3 and 7 post-injury, increased the M2 macrophages phenotype at day 7 post-CTX-induced injury *in vivo*, and promoted the M2 over M1 macrophage phenotypic polarization *in vitro*. Furthermore, hFL-OPG-Fc also improved muscle integrity *in vivo*, increased fiber cross-sectional area (CSA), and promoted regeneration and satellite cell density in the soleus (Sol) muscle at day 7 post-CTX injury. In addition, *in vivo* and *in vitro* hFL-OPG-Fc treatment increased the expression of β3 integrin, an important regulator of myogenic gene expression and satellite cell migration.[23] The hFL-OPG-Fc treatment also improved myotube maturation and fusion and decreased CTX-induced cytotoxicity and apoptosis *in vitro*. These findings thus demonstrate that hFL-OPG-Fc has the potential to attenuate muscle injury, promote cell survival, and improve muscle repair and regeneration.

RESULTS

An hFL-OPG-Fc treatment improved the force of CTX-injured Sol muscles

We used a severe CTX-induced muscle injury model to determine whether hFL-OPG-Fc had an impact on muscle repair. No differences were observed between phosphate-buffered saline (PBS)-treated and hFL-OPG-Fc-treated mice at day 3 post-injury where both displayed more than 85% loss in absolute and specific forces (Figures 1A and 1B, respectively). However, the hFL-OPG-Fc treatment significantly improved the isometric (P_0) and specific (sP_0) forces of the Sol

Table 1. Morphological and contractile properties of soleus (Sol) muscles at 7 days after CTX injection

	Sol					
Group	Mouse mass (g) ± SEM	Muscle mass (mg) ± SEM	L_0 (mm) ± SEM	Pt (g) ± SEM	$^1/_2$ RT (ms) ± SEM	TPT (ms) ± SEM
Sham	28.6 ± 2.0	8.1 ± 0.3	12.3 ± 0.3	3.7 ± 0.4	42.6 ± 3.4	36.6 ± 2.2
CTX-PBS	25.7 ± 0.6	6.2 ± 0.3**	11.3 ± 0.4	2.3 ± 0.2**	45.0 ± 2.8	35.6 ± 1.6
CTX-hFL-OPG-Fc	25.7 ± 0.6	6.2 ± 0.3**	11.6 ± 0.2	2.8 ± 0.2	41.6 ± 2.8	34.8 ± 2.4

The Sol muscles were incubated *ex vivo* in a controlled physiological environment (Krebs-Ringer solution supplemented with 95% O_2 and 5% CO_2, pH 7.4) at 25°C. L_0 values were determined, and the twitch tension (Pt), half-relaxation time ($^1/_2$ RT), and time to peak tension (TPT) were recorded. The muscle masses of Sol muscles from CTX-treated mice were significantly lower than those of Sol muscles from sham mice, while the Pt was significantly lower only in the PBS-treated group. No other morphological and contractile parameters were significantly different. Data are expressed as means ± SEM. **$p < 0.01$, indicate significantly different from sham mice using a one-way analysis of variance ANOVA with a Dunnett's test (one-way ANOVA) for multiple comparisons (n = 7–9).

muscles by 29% and 30%, respectively, compared to PBS at day 7 post-CTX-induced injury (Figures 1A and 1B). The force-frequency curve at day 7 shows that the hFL-OPG-Fc treatment increased tetanic forces selectively between 80 and 150 Hz (Figure 1C). Sol muscle masses from CTX-treated mice were significantly lower than those of Sol muscles from sham mice while twitch force (Pt) was significantly diminished only in the PBS-treated muscles (Table 1). No other morphological and contractile parameters were significantly different (Table 1).

An hFL-OPG-Fc treatment significantly improved muscle integrity and fiber CSA in Sol muscles at day 7 post-CTX injury

We determined whether hFL-OPG-Fc attenuates the severity of CTX-induced muscle damage. Cryosections of Sol muscles from C57BL/10J mice injected with CTX and treated with either vehicle (PBS) or hFL-OPG-Fc for 3 or 7 days were stained with hematoxylin and eosin (H&E) to evaluate muscle integrity. At day 3 post-injury, the area occupied by myofibers in Sol muscle was slightly higher, but statistically not significant, in hFL-OPG-Fc-treated compared with the PBS-treated mice (33% ± 7% versus 20% ± 7% of the total area, respectively; Figures 2A and 2B). However, an hFL-OPG-Fc treatment markedly increased the surface area occupied by myofibers compared to PBS-treated mice at day 7 post-CTX injury (74% ± 5% versus 57% ± 5% total area, respectively; Figures 2A and 2B). Furthermore, the fiber CSA of Sol muscles was significantly higher in the hFL-OPG-Fc-treated muscles than in the PBS control muscles at day 7 post-CTX-induced injury (1,100 ± 60 μm^2 versus 760 ± 96 μm^2, respectively; Figure 2C). The variance coefficient of the muscle fiber CSA determined using the minimal Feret's diameter method showed no difference in the muscle fiber heterogenicity of hFL-OPG-Fc-treated and PBS-treated mice at day 7 post-CTX-induced injury (238 ± 13 versus 246 ± 16, respectively; Figure 2D).

An hFL-OPG-Fc treatment significantly reduced neutrophil infiltration at 3 and 7 days post-injury and promoted M2 macrophage phenotype at 7 days following cardiotoxin-induced muscle damage

To assess the inflammatory response, injured Sol muscle sections from PBS- and hFL-OPG-Fc-treated mice were labeled with anti-Ly6-G/C, a marker for neutrophils (Figure 3A). The hFL-OPG-Fc treatment significantly reduced the number of neutrophils in Sol muscles compared to PBS-treated mice at day 3 (14,949 ± 988 versus 25,119 ± 3,164 cells/mm^3, respectively; Figure 3B) and at day 7 post-CTX injury (1,993 ± 473 versus 7,418 ± 829 cells/mm^3, respectively; Figure 3B). Neutrophil levels were significantly lower on day 7 post-injury in both hFL-OPG-Fc- and PBS-treated mice compared to day 3 post-injury (1,993 ± 473 versus 14,949 ± 988 cells/mm^3 for hFL-OPG-Fc-treated mice and 7,418 ± 829 versus 25,119 ± 3,164 cells/mm^3 for PBS-treated mice; Figure 3B). We then assessed the impact of an hFL-OPG-Fc treatment on pro-(M1) and anti-(M2) inflammatory macrophage infiltration on 3 and 7 days post-CTX-induced injury (Figure 3C). Total macrophage density, which includes M1 and M2 macrophages, had the tendency to be higher in hFL-OPG-Fc-treated mice at 7 days post-injury than in PBS control muscles (8,400 ± 2,465 versus 4,688 ± 1,040 cells/mm^3, respectively, Figure 3D). M1 macrophage ($F4/80^+/CD206^-$) levels were significantly lower on day 7 post-injury in hFL-OPG-Fc-treated mice compared to day 3, while they were lower but statistically not significant in PBS-treated mice (2,366 ± 345 versus 969 ± 244 cells/mm^3 for hFL-OPG-Fc-treated mice and 2,673 ± 957 versus 1,637 ± 547 cells/mm^3 for PBS-injected mice; Figure 3E). No significant difference was observed in M1 density between PBS-treated and hFL-OPG-Fc-treated mice at day 3 and day 7 post-injury (Figure 3E). Interestingly, at day 7 post-injury, the number of M2 macrophages ($F4/80^+/CD206^+$) increased significantly (+49%) in hFL-OPG-Fc-treated mice compared to PBS-treated mice (6,656 ± 1,518 versus 3,422 ± 618 cells/mm^3, respectively; Figure 3F). We also observed a significant increase in M2 macrophage density (+59%) in hFL-OPG-Fc-treated mice at day 7 post-injury compared to day 3 post-injury (Figure 3F).

An hFL-OPG-Fc treatment significantly improved muscle repair and regeneration

To better understand how hFL-OPG-Fc improves force production in injured Sol muscles, we examined the impact of an hFL-OPG-Fc treatment on muscle repair and regeneration following CTX-induced injury. hFL-OPG-Fc treatment significantly increased the average number of centrally nucleated myofibers at 7 days following injury (Figures 4A and 4B). Moreover, the CSA of centrally nucleated myofibers was significantly higher (+30%) in hFL-OPG-Fc-treated mice compared to those in the PBS group (1,138 ± 109 μm^2 versus 877 ± 41 μm^2, respectively; Figure 4C). To determine whether the

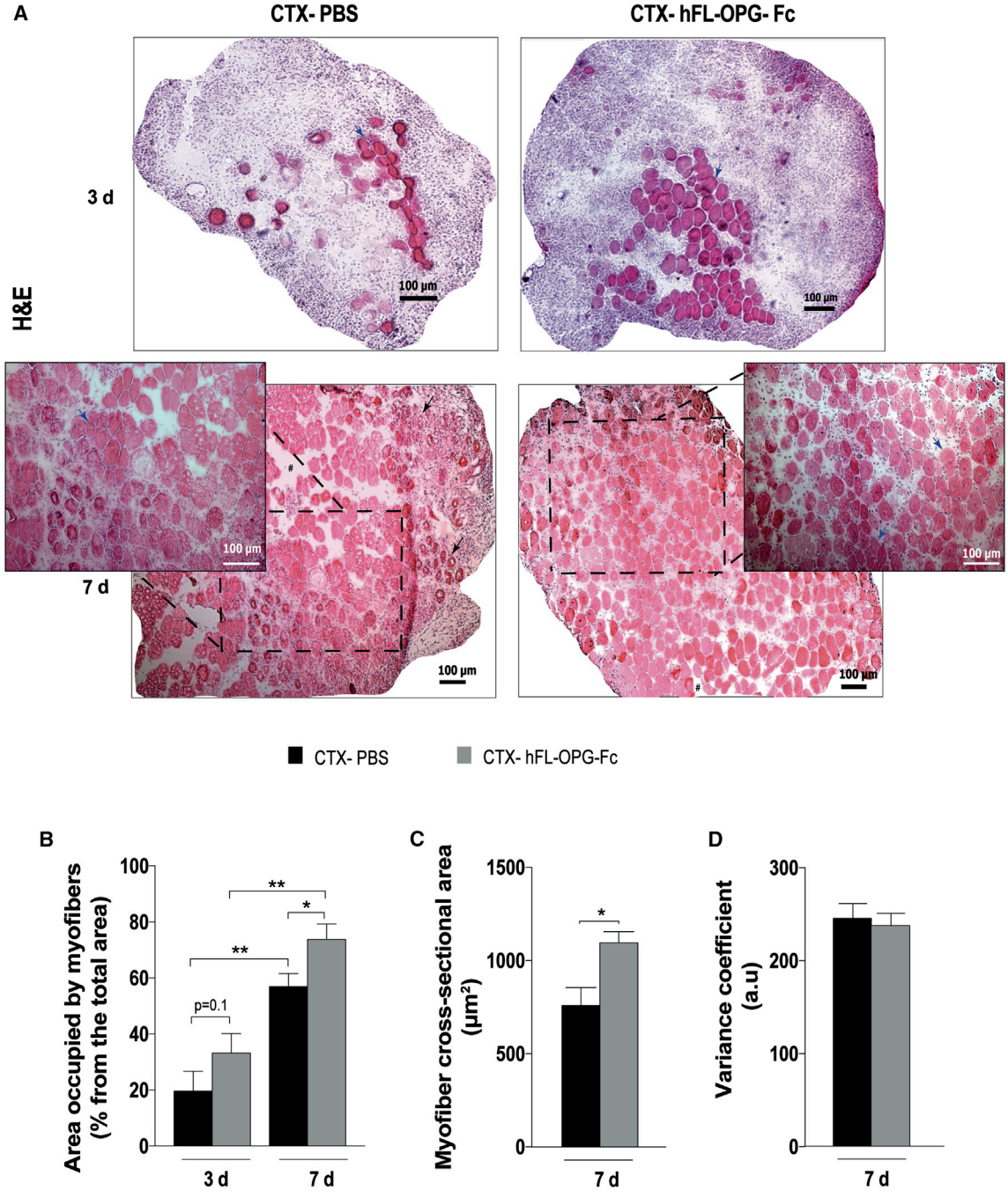

Figure 2. An hFL-OPG-Fc treatment significantly improved muscle integrity and fiber cross-sectional area (CSA) following cardiotoxin-induced muscle injury

(A) Images of hematoxylin and eosin (H&E)-stained Sol muscle sections from C57BL/10J mice injected with 15 µL of CTX (20 µM) followed by daily injections of either PBS or hFL-OPG-Fc (1 mg/kg/day) for 3 (n = 3–5) and 7 days (n = 6). The area occupied by myofibers was estimated using ImageJ 1.52a. (A and B) Three days after the CTX injection, the hFL-OPG-Fc-treated mice had slightly more myofibers than the PBS-treated mice (33% versus 20% of surface area occupied by myofibers, respectively). Seven days following CTX injection-induced injury, the area occupied by myofibers was significantly higher in Sol muscles from the hFL-OPG-Fc-treated mice than the PBS-treated mice. (C) Data are expressed as the percentage of myofiber area with respect to the total area. The myofiber CSA of Sol muscles at day 7 after the CTX injection was significantly higher in hFL-OPG-Fc-treated mice compared to PBS-treated mice. (D) The variance coefficient of the muscle fiber CSA determined using the minimal Feret's diameter method showed no difference in muscle fiber heterogenicity between hFL-OPG-Fc-treated and PBS-treated mice at day 7 post-CTX-induced injury. Complementary images

(legend continued on next page)

hFL-OPG-Fc treatment had an impact on satellite cell density, Sol muscle sections were immunolabeled with anti-Pax7 antibody, a marker for satellite cells. Sol muscle sections from hFL-OPG-Fc-treated mice displayed a significant increase in satellite cell density compared to PBS-treated mice (11,044 ± 1,271 versus 6381 ± 1035 cells/mm^3, respectively; Figures 4D and 4E). We next assessed the influence of hFL-OPG-Fc on regenerating muscles. Sol muscle sections were immunolabeled with anti-embryonic myosin heavy chain (e-MyHC) antibody, a marker for regenerating myofibers. A 7-day hFL-OPG-Fc treatment increased the average number of e-MyHC-positive myofibers by approximately 35% compared to PBS-treated mice (Figures 4F and 4G). We also determined whether an hFL-OPG-Fc treatment affects β3 integrin and myogenin levels in injured muscle since their expressions are increased during satellite cell differentiation, muscle regeneration,[23] and development.[24] A western blot (WB) analysis revealed that an hFL-OPG-Fc treatment significantly increased β3 integrin (+33%) and myogenin (+78%) protein levels in CTX-injured Sol muscles (Figures 4H and 4I).

An hFL-OPG-Fc treatment induced M2 macrophage polarization *in vitro*

M2 anti-inflammatory macrophages directly support myogenesis and myofiber growth by expressing very high levels of anti-inflammatory cytokines and growth factors such as transforming growth factor (TGF)-β, insulin-like growth factor I (IGF-I), and hepatocyte growth factor (HGF), which participate in the activation and stimulation of the differentiation of satellite cells.[14,25] Since M2 macrophage density was significantly increased in hFL-OPG-Fc-treated mice, we next assessed whether hFL-OPG-Fc directly promotes the M2 macrophage polarization using a murine J774 A.1 macrophage cell line *in vitro* (Figure 5A). Our results indicated that total macrophage density (F4/80+ cells) tended to be increased following hFL-OPG-Fc (200 ng/mL) treatment compared to PBS-treated J774 A.1 macrophages (21.1% ± 2.7% versus 15.3% ± 1.9%, respectively; Figure 5B). M1 macrophages (F4/80$^+$/CD206$^-$) were markedly reduced in hFL-OPG-Fc- compared to PBS-treated cells (1.8% ± 0.4% versus 2.9% ± 0.6%, respectively; Figure 5C) while hFL-OPG-Fc treatment induced a significant increase in M2 macrophages (F4/80$^+$/CD206$^+$) by 36% compared to PBS-treated J774 A.1 macrophages (19.3% ± 2.9% versus 12.4% ± 2,1%, respectively; Figure 5D). Interleukin (IL)-4/IL-13-treated cells were used as a positive control for M2 polarization. We also determined TNF-α and inducible nitric oxide synthase (iNOS) protein levels as M1 phenotype markers, and the anti-chitinase 3-like protein 3 + chitinase 3-like protein 4 (Ym1/2) as the M2 macrophage marker. Western blots results showed that 200 ng/mL hFL-OPG-Fc significantly decreased the expression of TNF-α (−20%; Figure 5E) and iNOS (−32%; Figure 5F), while Ym1/2 protein level significantly increased following hFL-OPG-Fc treatment (+30%; Figure 5G).

An hFL-OPG-Fc treatment enhanced C2C12 myotube maturation and attenuated CTX-induced cytotoxicity *in vitro*

We next assessed the effect of an hFL-OPG-Fc treatment on myotube maturation and fusion *in vitro*. Our results showed that hFL-OPG-Fc (200 and 1,000 ng/mL) induces myotube maturation and growth as indicated by an increase in the mean myotube diameter (Figures 6A and 6B). The myotube diameter distribution also shows that a 24-h treatment with hFL-OPG-Fc (50, 100, 200, and 1,000 ng/mL) reduced the number of small myotubes (5–10 μm in diameter) in a dose-dependent manner and that a high dose of hFL-OPG-Fc (1,000 ng/mL) significantly increased the number of large myotubes (>35 μm in diameter; Figure 6C). We also evaluated the fusion index (number of nuclei in myotubes/total number of nuclei) in the presence of hFL-OPG-Fc. hFL-OPG-Fc (1,000 ng/mL for 3 days) promoted myotube maturation and fusion, as indicated by the significant increase in the fusion index compared to PBS-treated myotubes (35% ± 1.7% versus 26% ± 2.1%, respectively; Figures 6D and 6E). We also investigated whether hFL-OPG-Fc attenuates CTX-induced cytotoxicity in myotubes. Our results show that the levels of lactate dehydrogenase (LDH) and creatine kinase (CK), two markers of muscle cell damage, were significantly reduced by more than 40% and 50%, respectively, in hFL-OPG-Fc-treated (from 100 to 1,000 ng/mL) myotubes (Figures 7A and 7B). To better understand how hFL-OPG-Fc reduces cytotoxicity, we investigated the capacity of hFL-OPG-Fc to prevent CTX-induced apoptosis. Western blot results show that 200 and 1,000 ng/mL hFL-OPG-Fc significantly decreased the expression of cleaved caspase-3 and Bax proteins (Figures 7C and 7D, respectively) while β3 integrin protein levels increased incrementally up to 2.5-fold following a treatment with 1000 ng/mL hFL-OPG-Fc (Figure 7E). Lastly, representative images of TUNEL (terminal deoxynucleotidyl transferase dUTP nick end labeling) immunofluorescence and combined quantitative data show that pretreating myotubes with 1,000 ng/mL hFL-OPG-Fc before exposing them to a 1-h CTX treatment resulted in a significant decrease in the number of TUNEL$^+$ apoptotic cells compared with PBS-treated myotubes (Figures 7F and 7G).

DISCUSSION

We previously used genetic and pharmacological approaches to show that muscle-specific *Rank* deletion, TR-OPG-Fc, and, to a larger extent, FL-OPG-Fc treatments restore muscle function in dystrophic mice.[16] Although a beneficial effect has been seen in the context of DMD, the potential use of hFL-OPG-Fc as an enhancer of muscle repair has never been tested. To translate the use of hFL-OPG-Fc into human clinical applications, we investigated the impact of hFL-OPG-Fc on muscle inflammation and repair following CTX-induced muscle damage. Our results show that an hFL-OPG-Fc treatment improved muscle force and integrity by reducing neutrophil infiltration in the early (day 3 post-injury) and mid-phase (day 7

of H&E staining of both hFL-OPG-Fc- and PBS-treated mice at 7 days post-CTX-induced injury are presented in Figures S2 and S3, respectively. Blue arrows indicate mature and regenerating myofibers. Black arrows and the hashtag, which indicate degenerating/necrotic myofibers and empty spaces, respectively, were excluded from quantification. Scale bars represent 100 μm. Data are expressed as means ± SEM. *$p < 0.05$ indicates significantly different from PBS-treated mice using the Student's t test (n = 3–6); **$p < 0.01$ indicates statistical differences between day 3 and day 7 for the respective treatment groups.

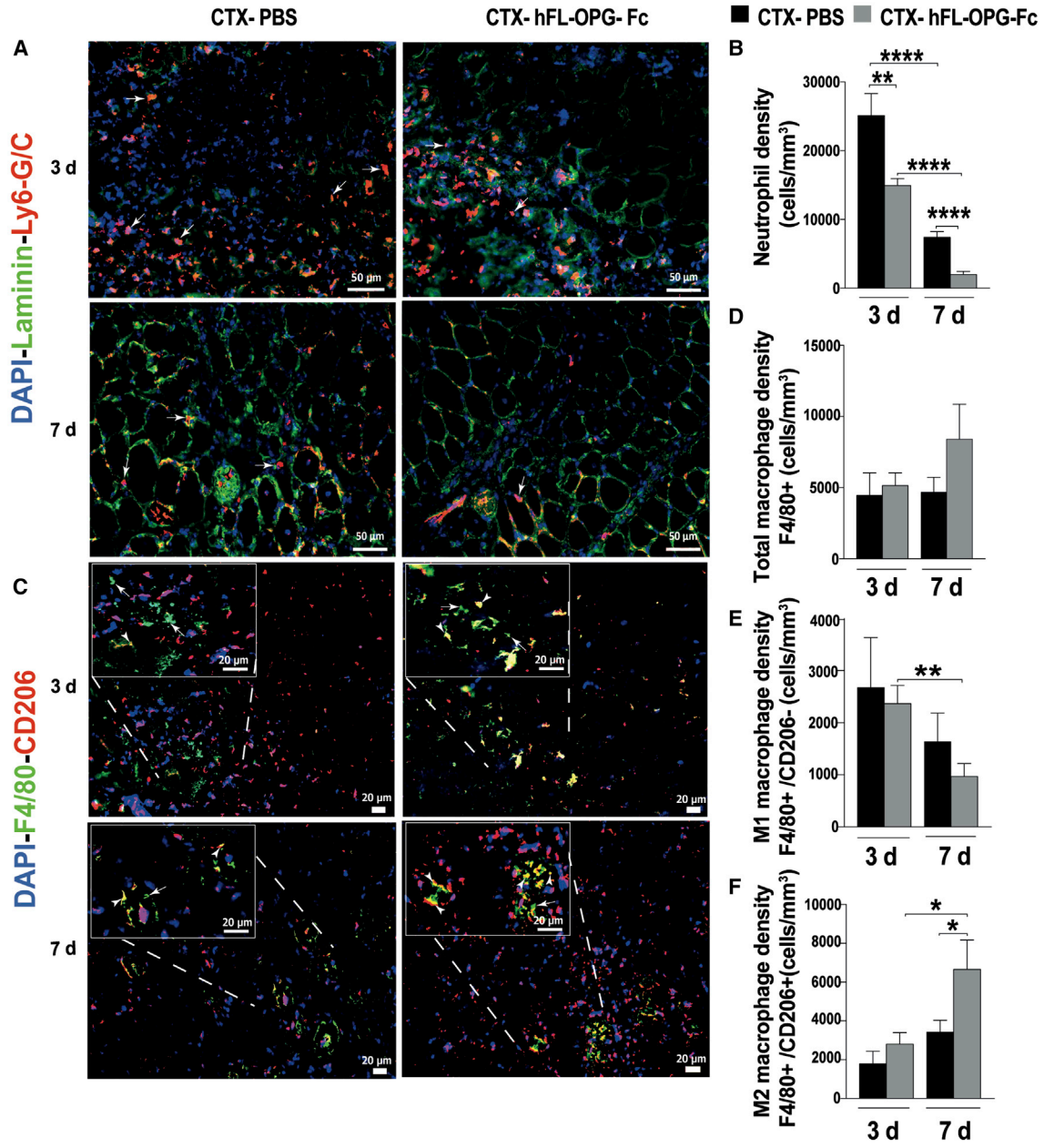

Figure 3. An hFL-OPG-Fc treatment significantly reduced neutrophil infiltration at 3 and 7 days post-injury and promoted M2 macrophage phenotype 7 days following cardiotoxin-induced muscle damage

(A) Sol muscle sections from C57BL/10J mice injected with 15 µL of CTX (20 µM) followed by daily injections of either PBS or hFL-OPG-Fc (1 mg/kg/day) for 3 (n = 4–5) or 7 (n = 5–6) days were labeled with anti-Ly6-G/C (red), anti-laminin (green), and DAPI (blue) to evaluate neutrophil infiltration. (A and B) An hFL-OPG-Fc treatment following CTX-induced Sol muscle injury significantly reduced the number of neutrophils at day 3 and day 7 post-injury compared to PBS-treated mice. Arrows show neutrophils in (A). (B) Both PBS- and hFL-OPG-Fc-treated mice exhibited a significant decrease in neutrophil infiltration at day 7 after the CTX injection compared to day 3 post-injury. (C) Anti-F4/80 (green) and anti-CD206 (red) were used to label all macrophage phenotypes and M2 macrophages, respectively, in Sol muscle sections at day 3 and day 7 post-injury. M1 macrophages are F4/80$^+$/CD206$^-$ (green) and are indicated by arrows. M2 macrophages are F4/80$^+$/CD206$^+$ (yellow) and are indicated by arrowheads. (D) At day 7 after muscle injury, total macrophages tended to be higher but not statically significant in hFL-OPG-Fc-treated mice compared to PBS-injected muscles. M1 macrophage (F4/80$^+$/CD206$^-$) levels were significantly lower at day 7 compared to day 3 post-injury in hFL-OPG-Fc-treated mice. (E) No significant differences were observed in M1 macrophage densities between PBS-treated and hFL-OPG-Fc-treated mice at both day 3 and 7 post-injury. (F) The number of M2 macrophages (F4/80$^+$/CD206$^+$) at day 7 was significantly higher in hFL-OPG-Fc-treated muscles compared to those from the PBS group. A significant increase in M2 macrophage density was observed in hFL-OPG-Fc-treated mice at day 7 compared to day 3 post-injury. Scale bars represent 50 µm in (A) and 20 µm in (C). Data are expressed as means ± SEM. *$p < 0.05$, **$p < 0.01$, and ****$p < 0.0001$ indicate significantly different using a Student's t test (n = 4–6).

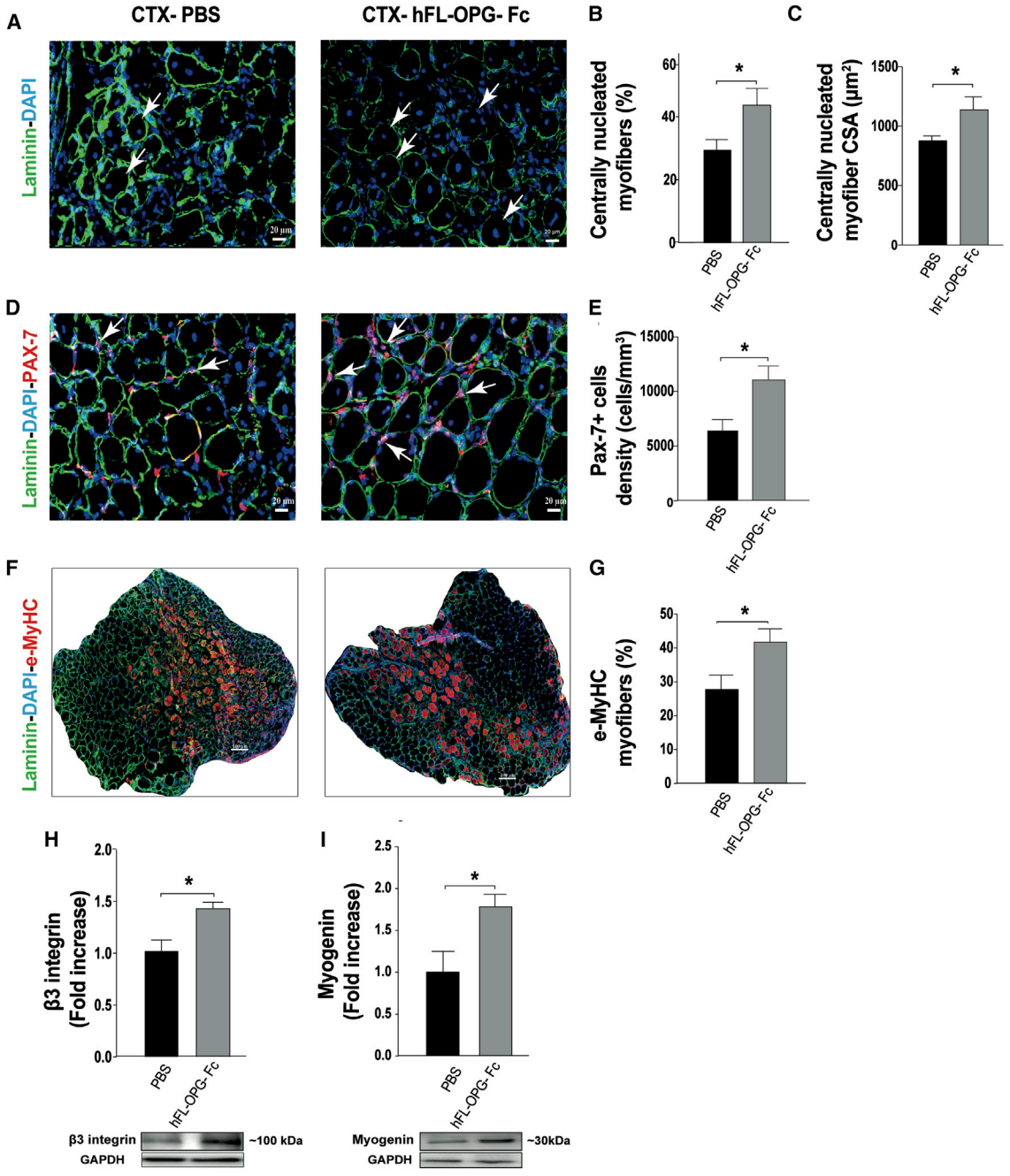

Figure 4. An hFL-OPG-Fc treatment significantly improved muscle regeneration and repair

(A, D, and F) Sol muscle sections were labeled with anti-laminin (green) and DAPI (blue) to evaluate centrally nucleated myofibers (n = 6, A); anti-Pax7 (red), which marks satellite cells (n = 8, D); and anti-MyH3 (red), which identifies e-MyHC (n = 6, F). (A, B, and C) Compared to a PBS injection, a 7-day treatment of cardiotoxin-injured muscles with hFL-OPG-Fc significantly increased the average number of centrally nucleated myofibers (A and B) and their CSA (C). (D–G) $Pax7^{+}$ cells co-localizing with DAPI (nuclei marker) indicating satellite cells (D and E) and e-MyHC myofibers (F and G) were significantly higher in hFL-OPG-Fc treated Sol muscles. (H and I) Western blot analyses showed that β3 integrin (H) and myogenin (I) protein levels in the Sol muscles were significantly higher following a 7-day hFL-OPG-Fc treatment. Protein levels were normalized to GAPDH content and are expressed as fold increase (n = 4). Arrows show centrally nucleated myofibers in (A) and Pax7-expressing cells in (D). Scale bars represent 20 μm in (A) and (D) and 100 μm in (F). Data are expressed as means ± SEM. *$p < 0.05$ indicates significantly different from the PBS-treated mice using Student's t test (n = 4–8).

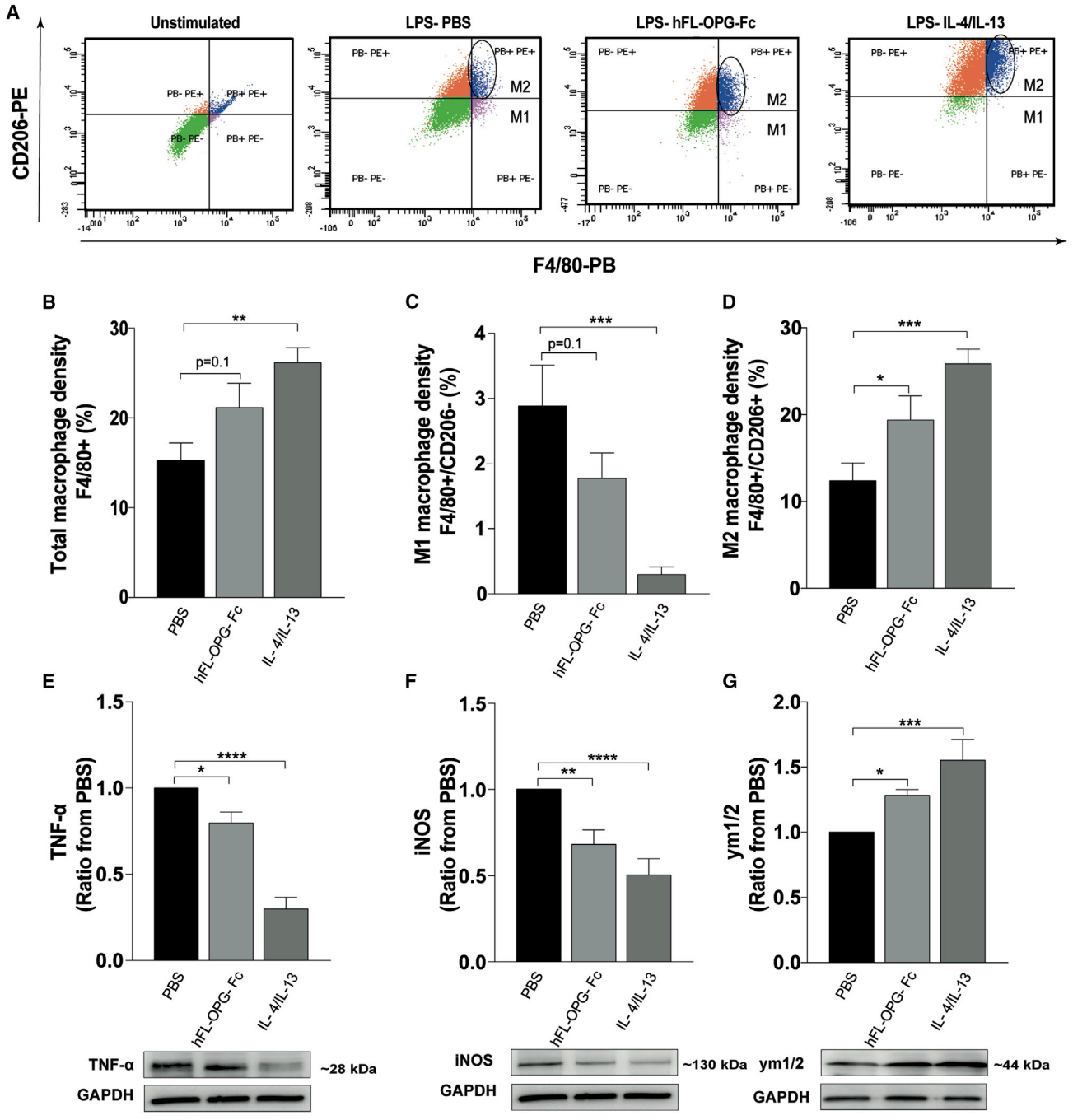

Figure 5. An hFL-OPG-Fc treatment induced M2 macrophage polarization *in vitro*

Murine macrophage cells were stimulated with LPS (1,000 ng/mL) followed by a 24-h treatment with either PBS, hFL-OPG-Fc (200 ng/mL), or both IL-4 and IL-13 (10 ng/mL of each) for M2 phenotype polarization. (A) To test whether hFL-OPG-Fc treatment induces M2 polarization, total macrophage and M2 phenotypes were labeled using F4/80 and CD206, respectively, and sorted by flow cytometry. (B–D) hFL-OPG-Fc treatment induced a slight increase in total macrophages ($F4/80^+$ cells) (B), a marked decrease in M1 macrophages ($F4/80^+/CD206^-$) (C), and a significant increase in M2 macrophages ($F4/80^+/CD206^+$) (D) compared to PBS-treated cells. (E and F) IL-4/IL-13-treated cells were used as a positive control for M2 polarization. The experiment was performed four separate times. Western blot results show that hFL-OPG-Fc significantly decreased TNF-α (E) and iNOS (F) proteins levels, both M1 macrophage markers. (G) The expression of chitinase 3-like 3 and 4 proteins (Ym1/2), an M2 macrophage marker, was significantly increased in hFL-OPG-Fc-treated cells. Protein levels were normalized to GAPDH content and expressed in ratio from PBS (n = 7–15). Data are expressed as means ± SEM. *$p < 0.05$, **$p < 0.01$, ***$p < 0.001$, and ****$p < 0.0001$ indicate significantly different from PBS using one-way ANOVA for multiple comparisons followed by a Dunnett's post hoc test.

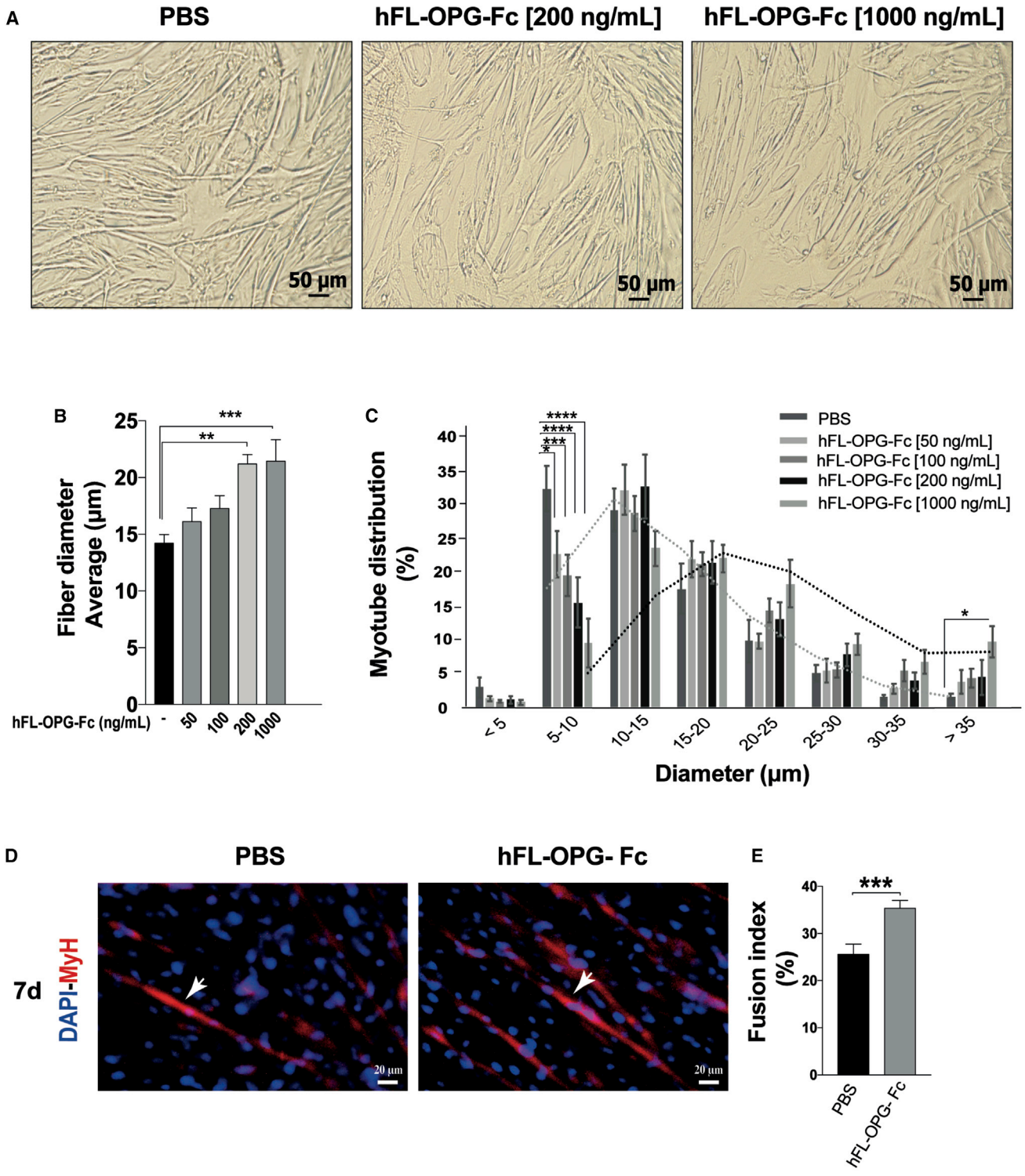

Figure 6. An hFL-OPG-Fc treatment improved myotube fusion and maturation *in vitro*

(A) Differentiated C2C12 myotubes were treated for 24 h with either PBS or different concentrations of hFL-OPG-Fc (50, 100, 200, or 1,000 ng/mL). Bright-field images were acquired at ×10 magnification. (B) hFL-OPG-Fc treatments (200 and 1,000 ng/mL) promoted myotube maturation, as indicated by the significant increase in fiber diameter following the treatments. (C) The distribution of myotube diameters showed that a 24-h hFL-OPG-Fc treatment significantly reduced the number of small myotubes (5–10 μm

(legend continued on next page)

post-injury) of muscle repair and by promoting, *in vivo*, an anti-inflammatory M2 macrophage phenotype and the regeneration process. *In vitro*, our results show that hFL-OPG-Fc promoted anti-inflammatory M2 macrophage phenotype and increased myotube maturation and fusion, attenuated CTX-induced cytotoxicity, and inhibited the apoptotic signaling pathway in differentiated C2C12 myotubes.

A single intramuscular CTX injury induced 85% and 45% losses of specific muscle force at day 3 and day 7, respectively. These results are in line with the literature since injury induced by snake toxins can cause a large amount of damage, destroying nearly all fibers at the injury site,[26–28] with a concomitant significant loss of muscle-specific force.[29] A 7-day treatment with hFL-OPG-Fc increased the isometric and specific forces of Sol muscles by approximately 30%. These results are in line with our observations in dystrophic muscles that showed that FL-OPG-Fc mitigates the loss of muscle force in a dose-dependent manner and preserves muscle integrity,[5] in addition to being more efficacious at preserving muscle function than muscle-specific *Rank* deletion, TR-OPG-Fc (only RANKL-binding domains), or anti-RANKL,[16] suggesting that hFL-OPG-Fc is a multifunctional molecule and could potentially act in multiple ways, impacting different cellular processes during muscle repair.

Muscle damage and inflammation are the main hallmarks of thermal, chemical, and mechanical injuries. Although regeneration is very often complete 1 month after acute injury, the trajectories of the regenerative process vary and are largely dependent on the dose of myotoxin used and the extent of damage at the time of injury.[27] Our findings show the presence of neutrophils 3 days following injury in both experimental groups and, most importantly, hFL-OPG-Fc treatments significantly reduced their density 3 and 7 days post-injury compared to PBS. The presence of neutrophils at 3 days post-injury are in line with a previous study that reported that neutrophil concentrations can remain elevated in injured muscles for several days following myofiber damage.[27,30] Depending on the extent of the damage induced by CTX injection, neutrophil density increases within hours of injury and may remain high 4 days after injury.[27] Considering the extent of damage observed at an early stage, the persistence of neutrophils at day 3 post-injury is not surprising. Furthermore, our results show that neutrophil density fell by more than 70% and 87% in PBS- and h-FL-OPG-Fc-treated mice, respectively, between days 3 and 7. However, we did not determine whether hFL-OPG-Fc acts directly on neutrophil recruitment or fate or whether it is a consequence of improved muscle integrity and the regeneration process as previously reported in dystrophic muscles.[5] Our results demonstrate that hFL-OPG-Fc treatments significantly increased anti-inflammatory M2 macrophage density and improved muscle fiber CSA at 7 days post-injury. M2 macrophages are important for dampening environmental inflammatory signals and supporting myogenesis and myofiber growth.[14] M2 macrophage depletion at an advanced stage induces a decrease in myofiber CSA, which correlates with the absence of effective muscle growth.[25] These findings support our results showing that the rise in M2 macrophage density is associated with better regeneration following hFL-OPG-Fc treatment. Furthermore, we demonstrated that hFL-OPG-Fc treatment promoted the M2 over M1 phenotypic polarization in culture. Mechanistically, we speculate that hFL-OPG-Fc may inhibit RANKL *in vivo* since we have previously demonstrated that the anti-RANKL treatment increased the proportion of anti-inflammatory and non-cytotoxic M2 macrophages in dystrophic mice[17] and that M2 macrophage polarization occurred via inhibition of the NF-κB signaling pathway in the J774A.1 macrophage cell line.[31] Although, we cannot exclude the potential effect of endogenous OPG in the current model of muscle injury, hFL-OPG-Fc treatments had significant effects compared to control PBS treatments in mice. In addition, our *in vitro* results show that hFL-OPG-Fc protected myotubes from CTX-induced injury, as the myotubes were devoid of inflammatory cells. As CTX-induced muscle damage is first initiated by a Ca^{2+} overload,[32] and as we previously showed that mFL-OPG-Fc increases SERCA (sarco/endoplasmic reticulum Ca^{2+} ATPase) activity and expression, a key regulator of Ca^{2+} homeostasis,[16] the *in vitro* and *in vivo* results from the present study support the notion that an hFL-OPG-Fc treatment could potentially influence intracellular Ca^{2+} dynamics following CTX injury. Overall, hFL-OPG-Fc protects the integrity of myofibers by reducing the number of inflammatory cells and the extent of muscle damage, thereby improving the function of injured muscles.

Skeletal muscles have a great capacity for repair and regeneration in response to injury. This capacity for regeneration is largely due to satellite cells, a myogenic stem cell population in adult skeletal muscles.[33] We demonstrate that a 7-day treatment with hFL-OPG-Fc increased satellite cell density in damaged areas of muscles ($Pax7^+$ cells). Consistent with this observation, others have reported that OPG promotes cell survival, proliferation, and migration by its interaction with heparin-binding domains and heparan sulfate proteoglycans (HSPs).[19,34] Interestingly, HSPs are highly expressed in regenerating myofibers and satellite cells and are linked to various signaling pathways involved in myogenesis, differentiation, and adhesion.[35] Additionally, the increase in satellite cell density resulting from an hFL-OPG-Fc treatment may also occur via αvβ3 or αvβ5 integrin, as the inhibition of αvβ3 or αvβ5 integrin with monoclonal antibodies attenuates OPG-induced mobilization and proliferation in human microvascular endothelial cells.[21] Furthermore, β3 integrin

in diameter) in a dose-dependent manner and increased the number of large myotubes (>35 μm in diameter) at the highest dose of hFL-OPG-Fc used (1,000 ng/mL). (D) We also evaluated the fusion index (number of nuclei in myotubes/total number of nuclei) in the presence of hFL-OPG-Fc. C2C12 myotubes were treated with either PBS or hFL-OPG-Fc (1,000 ng/mL) for 3 days beginning on day 1 of differentiation and were then immunolabeled with anti-MyHC (myosin heavy chain; red) and DAPI (nuclei; blue). (D and E) The hFL-OPG-Fc treatments promoted myotube maturation and fusion, as indicated by the significant increase in fusion index following the hFL-OPG-Fc treatment. Scale bars represent 50 μm in (A) and 20 μm in (D). Data are expressed as means ± SEM. *$p < 0.05$, **$p < 0.01$, ***$p < 0.001$, and ****$p < 0.0001$ indicate significantly different from PBS using an analysis of variance with a Dunnett's test (one- or two-way ANOVA) for multiple comparisons (n = 6).

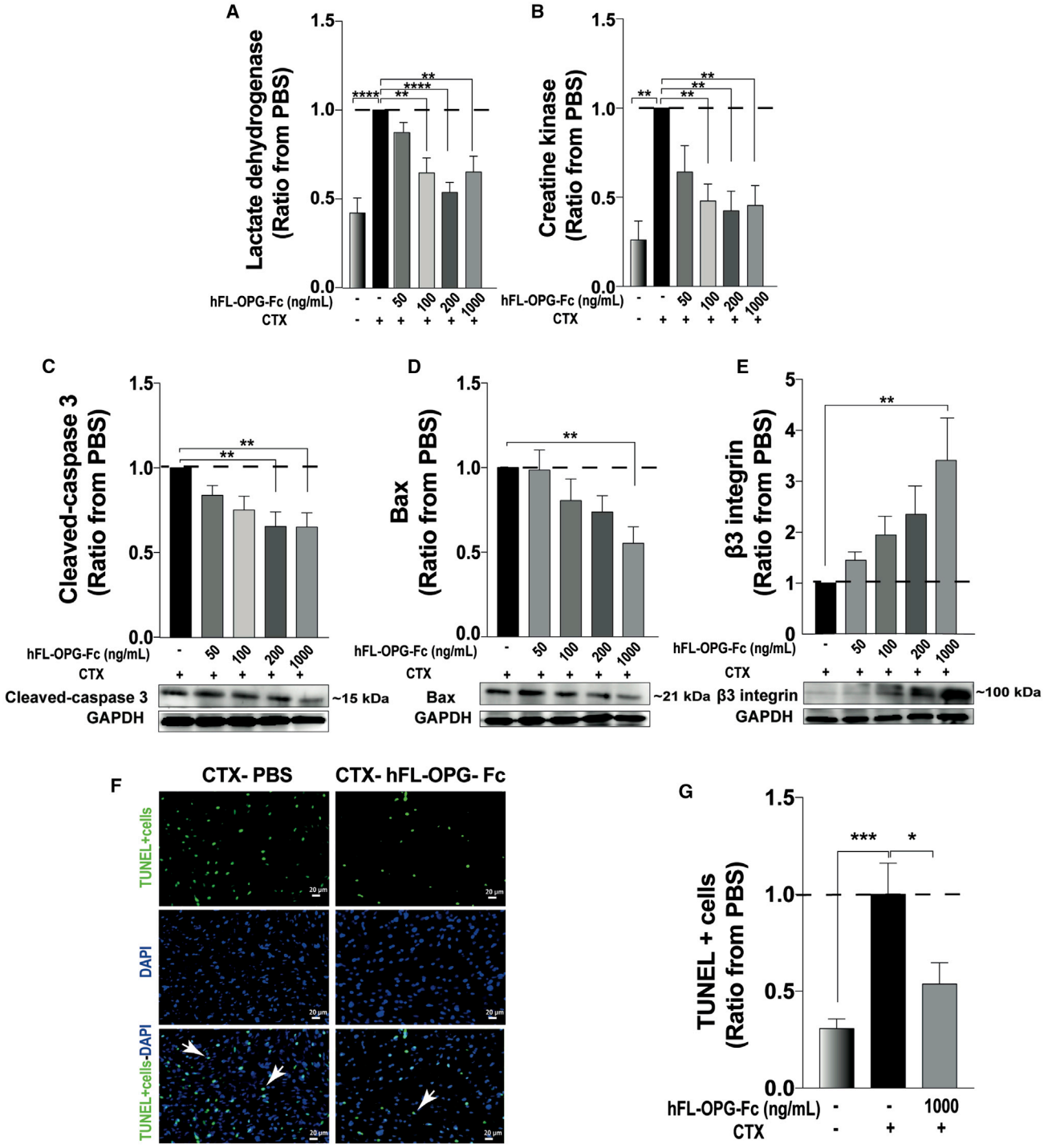

Figure 7. An hFL-OPG-Fc treatment attenuated cardiotoxin-induced cytotoxicity and apoptosis in differentiated C2C12 myotubes *in vitro*

Differentiated C2C12 myotubes were treated for 24 h with hFL-OPG-Fc (50, 100, 200, and 1,000 ng/mL) and were then exposed to CTX (1 μM) for 1 h. Supernatants were collected from the wells, and lactate dehydrogenase (LDH) and creatine kinase (CK) assays were performed to evaluate myotube integrity (n = 10). The hFL-OPG-Fc treatments (100–1,000 ng/mL) attenuated CTX-induced cell cytotoxicity, as shown by the significantly lower LDH and CK levels in myotubes treated with hFL-OPG-Fc. (A and B) The LDH and CK results are presented as the ratio between hFL-OPG-Fc-treated and untreated myotubes. (C–E) Representative images of western blots and their quantification show that the levels of cleaved caspase-3 and Bax proteins were significantly decreased (C and D) while the level of β3 integrin protein was significantly increased (E) after the hFL-OPG-Fc treatments. Protein levels were normalized to GAPDH content and are expressed as either a ratio or fold changes from PBS-treated

(legend continued on next page)

expression is increased during satellite cell differentiation and muscle regeneration.[23] Our results show that β3 integrin protein expression was higher in regenerating Sol muscles and in myotubes treated with hFL-OPG-Fc, which supports our data showing that hFL-OPG-Fc increased satellite cells density and enhanced muscle regeneration through the integrin signaling pathway. In line with this observation, the numbers of centrally nucleated cells and e-MyHC myofibers, two markers of myogenesis and repair, were significantly increased following an hFL-OPG-Fc treatment. Although the expression of e-MyHC is initiated at 3 days and may persist for up to 14 days after injury in the Sol muscle,[36,37] the increase in myofibers expressing e-MyHC following hFL-OPG-Fc treatment strongly supports a better regeneration since the e-MyHC expression correlates with the increase in contractile tissue, as represented by the area occupied by myofibers. While we cannot exclude other signaling pathways, our results and the literature suggest that OPG, with its three different binding domains (RANKL, TRAIL, and heparin), could directly or indirectly influence the regeneration of myofibers through the HSP and integrin pathways.

In addition to preserving muscle integrity, hFL-OPG-Fc also dose-dependently improved the maturation and fusion and prevented the death of myotubes *in vitro*, which supports our *in vivo* findings. Our *in vitro* results also show that β3 integrin was highly expressed and that the expression of pro-apoptotic proteins such as cleaved caspase-3 and Bax was reduced, shedding some light on the mechanism of action of hFL-OPG-Fc. In line with these observations, β3 integrin is transiently upregulated during myotube differentiation and is highly involved in myoblast migration and myotube differentiation, while its inhibition impairs myogenic gene expression and myotube formation.[23] In addition, OPG possesses a decoy receptor for TRAIL, preventing cell death ensuing from the activation of caspase-3 and other pro-apoptotic proteins such as Bax.[38] Other pharmacological experiments have shown that OPG can directly bind to αvβ3 and αvβ5 integrins and promote cell survival.[39] Although further experiments are warranted to evaluate the off-target role of FL-OPG-Fc in skeletal muscle, these findings indicate that hFL-OPG-Fc promotes myotube growth and attenuates cell death *in vitro* through a mechanism that is to some extent independent of RANKL inhibition.

In conclusion, we show for the first time that hFL-OPG-Fc modulates the inflammatory response, increases satellite cell density and muscle regeneration, and ultimately improves muscle force production and integrity. Our *in vitro* results show that hFL-OPG-Fc promotes M2 macrophage phenotype, improves muscle cell maturation and fusion, and attenuates apoptosis. Altogether, our findings demonstrate that hFL-OPG-Fc protects Sol muscle by limiting damage and promoting repair following acute injury, hence its potential for clinical applications for diseases in which muscle repair and regeneration are impaired.

MATERIALS AND METHODS

Animals

All animal experiments were approved by the Université Laval Research Center Animal Care and Use Committee based on Canadian Council on Animal Care guidelines. Male wild-type (WT; C57BL/10J) mice were purchased from The Jackson Laboratory. Food and water were provided *ad libitum*. Mice were screened for the desired genotype by PCR analysis. At the end of the different experimental procedures, the mice were euthanized by cervical dislocation under anesthesia. All experiments, data acquisition, and analyses were performed by "blinded" experimenters.

CTX-induced muscle injury

Male WT (C57BL/10J) mice were used at 10–12 weeks of age. They were anesthetized with isoflurane inhalation and were injected with slow-release buprenorphine (0.1 mg/kg) to alleviate pain. The right and left hindlimbs were shaved prior to the CTX-induced muscle injury. A small incision (5 mm) was performed on the lateral side of each leg to expose the Sol muscles. CTX (total volume of 15 μL, 20 μM) from *Naja pallida* (Latoxan, Valance, France) was injected intramuscularly at three sites (5 μL per site at the distal, proximal, and mid-belly regions of each Sol muscle). Sham mice were operated but did not receive the intramuscular CTX injections. Following the CTX injections, the C57BL/10J mice were treated for 3 or 7 days with intraperitoneal (i.p.) injections of either vehicle (PBS) or hFL-OPG-Fc (1 mg/kg/day; National Research Council of Canada [NRCC]). A 3-day treatment was selected to evaluate the role played by hFL-OPG-Fc during the early inflammatory response, and a 7-day treatment was used to access its effects on muscle regeneration while limiting possible immune reactions to the fused protein. The mice were then euthanized. The right hindlimb Sol muscle was used to measure *ex vivo* contractile properties, and the left hindlimb Sol muscle was frozen for western blot and immunohistochemistry analyses.

Skeletal muscle contractile properties

The mice were injected subcutaneously (s.c.) with buprenorphine (0.1 mg/kg) and were anesthetized by an i.p. injection of pentobarbital sodium (50 mg/kg). The Sol muscle was gently removed, incubated at 25°C in Krebs-Ringer physiological solution (pH 7.4) supplemented with 95% O_2 and 5% CO_2, and attached to an electrode with a force sensor (305B-LR; Aurora Scientific, Aurora, ON, Canada). Contractile properties were measured using a 305B-LR dual-mode muscle arm system monitored by a dynamic muscle data acquisition and analysis system (Aurora Scientific). Maximum specific tetanic tension (sP_0; in N/cm^2) values were obtained by normalizing the absolute force (P_0) to the fiber CSA using the following

myotubes (n = 8). (F) Representative images of TUNEL immunofluorescence show the numbers of TUNEL$^+$ apoptotic cells in untreated and hFL-OPG-Fc-treated (1,000 ng/mL) myotubes following a 1-h exposure to CTX. (F and G) A 24-h treatment with hFL-OPG-Fc (1,000 ng/mL) induced a significant decrease in the number of TUNEL$^+$ apoptotic cells after a 1-h exposure to CTX compared with PBS-treated myotubes (n = 4). Scale bars represent 20 μm in (F). Data are expressed as means ± SEM. *$p < 0.05$, **$p < 0.01$, ***$p < 0.001$, and ****$p < 0.0001$ indicate significantly different from controls by analysis of variance for multiple comparisons with a Dunnett's test (n = 4–10).

equation: $sP_0 = P_0/CSA$. CSA was determined by dividing the muscle mass by the product of the optimum fiber length (Lf) corresponding to the result of multiplying optical length (L_0) with the fiber length ratio (0.71 for Sol muscles) and the muscle density (1.06 mg/mm^3). Muscle contractility results were analyzed using Dynamic Muscle Data Analysis software (Aurora Scientific).

Immunohistochemistry

Sol muscle cross-sections from PBS-treated and hFL-OPG-Fc-treated mice were washed for 5 min with PBS, fixed for 10 min with 4% paraformaldehyde (PFA), blocked with 5% BSA, 1% horse serum (HS) solution, and then incubated overnight at 4°C with the following primary antibodies: anti-laminin (Sigma-Aldrich, Oakville, ON, Canada, 1:250), anti-e-MyHC (F1.652 MYH3; DSHB, University of Iowa, Iowa City, IA, USA), anti-Pax7 (R&D Systems, Oakville, ON, Canada, 1:100), anti-Ly6-G/C (BD Biosciences, Mississauga, ON, Canada, 1:300), anti-F4/80 (Bio-Rad, Mississauga, ON, Canada, 1:100), and anti-CD206 (Santa Cruz, Dallas, TX, USA, 1:50) diluted in blocking solution. The sections were washed three times for 15 min with PBS and were incubated with Alexa Fluor 488- or 594-conjugated secondary antibodies (Invitrogen, Burlington, ON, Canada, 1:500) for 1 h at room temperature. The sections were washed three times for 15 min with PBS, mounted with DAPI Fluoromount-G (SouthernBiotech, Birmingham, AL, USA), and immunofluorescence labeling was analyzed using an Axio Imager M2 microscope (Zeiss) connected to an AxioCam camera using ZEN 2 software (Zeiss). Additional sections were stained with H&E according to the manufacturer's protocol (Sigma-Aldrich, Oakville, ON, Canada) to assess muscle integrity.

Immunohistochemistry analyses

For muscle regeneration analyses, two tiles per muscle were randomly selected from the distal and proximal regions and were analyzed. The results are presented as percentages based on the number of total fibers per tile. Satellite cells were quantified from at least six fields acquired using a ×20 objective, and data are presented as cell density (number of cells/mm^3). Muscle integrity was evaluated by measuring the area occupied by mature and regenerating myofibers, excluding empty spaces, degenerating, and necrotic myofibers, in two tiles per muscle randomly selected from the distal and proximal regions. The area occupied by mature and regenerating myofibers was measured by deducting the area not occupied by fibers analyzed from an image acquired using a ×10 objective using ImageJ software (version 1.41) from the total area, excluding artifacts resulting from the tissue preparation. Results are expressed as the percentage of myofiber area with respect to the total area. Images used for representing data were acquired using a ×20 objective and ×10 objective for tiles.

In vitro macrophage polarization

The murine J774 A.1 macrophage cell line kindly provided by Dr. Jacques Corbeil Laboratory, Centre de Recherche du CHU de Quebec–CHUL were cultured in high-glucose DMEM (Wisent, Canada) supplemented with 10% FBS (HyClone, Thermo Fisher Scientific) and 1% antibiotic-antimycotic (Thermo Fisher Scientific) in a 5% CO_2 atmosphere at 37°C. For M2 phenotype polarization experiments, cells were seeded in six-well culture plates and simultaneously stimulated with lipopolysaccharide (LPS; 1,000 ng/mL) and treated for 24 h with either PBS, hFL-OPG-Fc (200 ng/mL), or both IL-4 and IL-13 (10 ng/mL for each). After the treatment, cells were harvested and used either for western blot or fluorescence-activated cell sorting (FACS) analyses. The experiment was performed four separate times.

FACS analysis

Murine J774 A.1 macrophage cells stimulated with LPS and treated for 24 h with either PBS, hFL-OPG-Fc, or both IL-4 and IL-13 were harvested, washed with PBS, and then centrifuged at 1,600 rpm for 5 min at room temperature. Cells were resuspended in 100 μL of FACS wash buffer (PBS 1×, 0,05% BSA, 1% EDTA) and preincubated with mouse BD Fc Block purified anti-mouse CD16/CD32 (BD Pharmingen, CA, USA, 1:200) at room temperature for 10 min. To labeled macrophages, cells were incubated with F4/80 Pacific Blue-conjugated rat anti-mouse (BioLegend, USA, 1:200). M2-macrophages were labeled with CD206 R-phycoerythrin-conjugated rat anti-mouse (Thermo Fisher Scientific, Canada, 1:200) at 4°C for 30 min. Appropriate isotypes were used (BioLegend and Thermo Fisher Scientific, Canada), and am ABC anti-mouse bead kit (Invitrogen) was used for adjusting compensation. Flow cytometry was performed with an EPICS XL (Beckman Coulter, Fullerton, CA, USA), and the cell analyses were performed using FlowJo software (BD Biosciences).

Cell cultures

C2C12 myoblasts (ATCC, Manassas, VA, USA) were cultured in high-glucose DMEM (HyClone, Thermo Fisher Scientific, Ottawa, ON, Canada) supplemented with 10% FBS (HyClone, Thermo Fisher Scientific) and 1% antibiotic-antimycotic (Thermo Fisher Scientific) in a 5% CO_2 atmosphere at 37°C. When the myoblasts reached 90% confluence, the medium was replaced with high-glucose DMEM supplemented with 1% fetal horse serum and 1% insulin-transferrin-sodium selenite (ITS), and the myoblasts were incubated for a further 5 days to allow them to differentiate into myotubes. At day 4 of differentiation, the myotubes were treated with PBS or hFL-OPG-Fc (50, 100, 200, or 1,000 ng/mL) for 24 h. Bright-field images from at least five different fields covering a total of 300 myotubes were acquired using a Zeiss microscope, and the distribution and diameters of the myotubes were determined using ImageJ. Results are presented as the average of at least six experiments per condition and are normalized to PBS-treated cells. In a separate experiment, after day 4 of differentiation, the myotubes were treated with hFL-OPG-Fc (50, 100, 200, or 1,000 ng/mL) for 24 h and were exposed to CTX (1 μM) for 1 h to evaluate cytotoxicity.

LDH and CK activity assays

Twenty-four hours after a single treatment with PBS or hFL-OPG-Fc (50, 100, 200, or 1,000 ng/mL), the cells were exposed to CTX (1 μM) for 1 h. The culture medium from each well was then collected and centrifuged, and LDH activity was determined using a commercial kit (Promega, Madison, WI, USA). Briefly, 10 μL of medium was diluted in 40 μL of fusion medium. CytoTox 96 reagent (50 μL,

Promega) was then added to the reaction mixture. After a 30-min incubation, 50 μL of stop solution was added, and LDH activity was measured 1 h later using a spectrophotometer at an OD of 490 nm. LDH levels in the hFL-OPG-Fc-treated wells were normalized to the PBS wells. In parallel, 20 μL of medium was used to assay CK activity using a commercial kit (VWR International, Edmonton, AB, Canada). Activity was measured using a spectrophotometer at an optical density (OD) of 560 nm. CK levels in the hFL-OPG-Fc treatment wells were normalized to CK levels in the PBS treatment wells.

Western blotting

Injured Sol muscles from the left hindlimbs were immediately frozen after dissection. The muscles were homogenized for 45 s on ice in radioimmunoprecipitation assay (RIPA) lysis buffer supplemented with a protease inhibitor cocktail (P8340; Sigma-Aldrich) and a phosphatase inhibitor cocktail (2 mM Na_3VO_4, 50 mM NaF, and 0.2 mM PMSF; Sigma-Aldrich) using a tissue homogenizer (PowerGen 125; Thermo Fisher Scientific). C2C12 cells were also lysed using RIPA buffer. The protein content of the lysates was determined using a bicinchoninic acid (BCA) protein assay kit (EMD Chemicals, Ottawa, ON, Canada). The homogenates were heated to 95°C in Laemmli buffer for 2 min, separated by SDS-PAGE, and transferred to polyvinylidene fluoride (PVDF) membranes (Bio-Rad). The membranes were blocked in 5% skim milk and were incubated overnight at 4°C with the following primary antibodies: anti-β3 integrin (ab119992; Abcam, Toronto, ON, Canada), anti-myogenin (ab1835; Abcam), anti-cleaved caspase-3 (AF835; R&D Systems, Oakville, ON, Canada), anti-Bax (ab32503; Abcam), anti-TNF-α (AB2148P; Sigma-Aldrich, ON, Canada), anti-iNOS (ab202417; Abcam, ON, Canada), anti-Ym1/2 (ab192029, Abcam, ON, Canada), and anti-GAPDH (Cell Signaling Technology, Danvers, MA, USA). The anti-GAPDH was diluted 1:5,000 and the other antibodies were diluted 1:1,000. The membranes were washed, incubated with the appropriate HRP-conjugated secondary antibodies, and visualized by chemiluminescence using the ECL Plus imaging system (PerkinElmer). Band densities were analyzed using Quantity One software (v4.6.6; Bio-Rad) and were normalized to GAPDH.

Fusion index

When the myoblasts reached 70% confluence, the medium was replaced with high-glucose DMEM supplemented with 1% fetal horse serum and 1% ITS, and the myoblasts were treated with either PBS or hFL-OPG-Fc (1,000 ng/mL) for 3 days. The wells were washed three times with PBS, fixed for 20 min with 4% PFA, permeabilized for 10 min with 0.1% Triton X-100, blocked for 30 min in 5% BSA-PBS, and exposed to primary antibodies against MyH (Santa Cruz, 1:200) overnight at 4°C. The cells were washed three times with PBS, and then secondary anti-rabbit Alexa Fluor 594 was added for 1 h at room temperature. The cells were then washed three times with PBS and were mounted with DAPI gel (SouthernBiotech) before being examined under an Axio Imager M2 microscope equipped with ZEN software (Zeiss, Germany). The fusion index number of nuclei in the myotubes per total number of nuclei was determined in at least four randomly selected fields per well. The experiments were repeated six times (n = 6).

TUNEL assay

After day 4 of differentiation, the myotubes were treated for 24 h with either PBS or hFL-OPG-Fc (1,000 ng/mL) and were exposed to CTX (1 μM) for 1 h to evaluate cell death. TUNEL staining for C2C12-treated cells was performed using an *In Situ* Cell Death Detection kit (Roche, Mannheim, Germany). TUNEL-positive cells were counted in four randomly selected fields in the wells. The experiments were repeated four times. This experiment was performed under blinded conditions.

Statistical analyses

All values are expressed as means ± SEM. The data were analyzed using either a Student's t test or Dunnett's post hoc test (one-way ANOVA or two-way ANOVA) using Prism (version 3.1). The levels of significance were set at $^{*}p < 0.05$, $^{**}p < 0.01$, $^{***}p < 0.001$, and $^{****}p < 0.0001$.

SUPPLEMENTAL INFORMATION

Supplemental information can be found online at https://doi.org/10.1016/j.omtm.2021.03.022.

ACKNOWLEDGMENTS

This work was supported by grants to J.F. from the Natural Sciences and Engineering Research Council of Canada (RGPIN-2016-05845) and Jesse's Journey.

AUTHOR CONTRIBUTIONS

Z.B., A.A., and J.F. conceived and designed the project. Z.B., D.H., and L.M. performed the experiments and analyzed the data. Z.B., A.A., and J.F. drafted the manuscript. All of the authors checked the manuscript for scientific content and contributed to the final drafting of the manuscript. All the authors read and approved the final manuscript.

DECLARATION OF INTERESTS

The authors declare no competing interests.

REFERENCES

1. Boyce, B.F., Xiu, Y., Li, J., Xing, L., and Yao, Z. (2015). NF-κB-mediated regulation of osteoclastogenesis. Endocrinol. Metab. (Seoul) *30*, 35–44.
2. Boyle, W.J., Simonet, W.S., and Lacey, D.L. (2003). Osteoclast differentiation and activation. Nature *423*, 337–342.
3. Bernardi, S., Fabris, B., Thomas, M., Toffoli, B., Tikellis, C., Candido, R., Catena, C., Mulatero, P., Barbone, F., Radillo, O., et al. (2014). Osteoprotegerin increases in metabolic syndrome and promotes adipose tissue proinflammatory changes. Mol. Cell. Endocrinol. *394*, 13–20.
4. Tisato, V., Secchiero, P., Rimondi, E., Gianesini, S., Menegatti, E., Casciano, F., Zamboni, P., and Zauli, G. (2013). GM-CSF exhibits anti-inflammatory activity on endothelial cells derived from chronic venous disease patients. Mediators Inflamm. *2013*, 561689.
5. Dufresne, S.S., Dumont, N.A., Bouchard, P., Lavergne, É., Penninger, J.M., and Frenette, J. (2015). Osteoprotegerin protects against muscular dystrophy. Am. J. Pathol. *185*, 920–926.

6. Philippou, A., Bogdanis, G., Maridaki, M., Halapas, A., Sourla, A., and Koutsilieris, M. (2009). Systemic cytokine response following exercise-induced muscle damage in humans. Clin. Chem. Lab. Med. *47*, 777–782.

7. Rutti, S., Dusaulcy, R., Hansen, J.S., Howald, C., Dermitzakis, E.T., Pedersen, B.K., Pinget, M., Plomgaard, P., and Bouzakri, K. (2018). Angiogenin and osteoprotegerin are type II muscle specific myokines protecting pancreatic beta-cells against proinflammatory cytokines. Sci. Rep. *8*, 10072.

8. Hamoudi, D., Bouredji, Z., Marcadet, L., Yagita, H., Landry, L.-B., Argaw, A., and Frenette, J. (2020). Muscle weakness and selective muscle atrophy in osteoprotegerin-deficient mice. Hum. Mol. Genet. *29*, 483–494.

9. Dufresne, S.S., Frenette, J., and Dumont, N.A. (2016). [Inflammation and regeneration, a double-edged sword]. Med. Sci. (Paris) *32*, 591–597.

10. Teixeira, C.F.P., Zamunér, S.R., Zuliani, J.P., Fernandes, C.M., Cruz-Hofling, M.A., Fernandes, I., Chaves, F., and Gutiérrez, J.M. (2003). Neutrophils do not contribute to local tissue damage, but play a key role in skeletal muscle regeneration, in mice injected with *Bothrops asper* snake venom. Muscle Nerve *28*, 449–459.

11. Scapini, P., Lapinet-Vera, J.A., Gasperini, S., Calzetti, F., Bazzoni, F., and Cassatella, M.A. (2000). The neutrophil as a cellular source of chemokines. Immunol. Rev. *177*, 195–203.

12. Iwahori, Y., Ishiguro, N., Shimizu, T., Kondo, S., Yabe, Y., Oshima, T., Iwata, H., and Sendo, F. (1998). Selective neutrophil depletion with monoclonal antibodies attenuates ischemia/reperfusion injury in skeletal muscle. J. Reconstr. Microsurg. *14*, 109–116.

13. Locati, M., Mantovani, A., and Sica, A. (2013). Macrophage activation and polarization as an adaptive component of innate immunity. Adv. Immunol. *120*, 163–184.

14. Chazaud, B., Brigitte, M., Yacoub-Youssef, H., Arnold, L., Gherardi, R., Sonnet, C., Lafuste, P., and Chretien, F. (2009). Dual and beneficial roles of macrophages during skeletal muscle regeneration. Exerc. Sport Sci. Rev. *37*, 18–22.

15. Stout, R.D., Jiang, C., Matta, B., Tietzel, I., Watkins, S.K., and Suttles, J. (2005). Macrophages sequentially change their functional phenotype in response to changes in microenvironmental influences. J. Immunol. *175*, 342–349.

16. Dufresne, S.S., Boulanger-Piette, A., Bossé, S., Argaw, A., Hamoudi, D., Marcadet, L., Gamu, D., Fajardo, V.A., Yagita, H., Penninger, J.M., et al. (2018). Genetic deletion of muscle RANK or selective inhibition of RANKL is not as effective as full-length OPG-fc in mitigating muscular dystrophy. Acta Neuropathol. Commun. *6*, 31.

17. Hamoudi, D., Marcadet, L., Piette Boulanger, A., Yagita, H., Bouredji, Z., Argaw, A., and Frenette, J. (2019). An anti-RANKL treatment reduces muscle inflammation and dysfunction and strengthens bone in dystrophic mice. Hum. Mol. Genet. *28*, 3101–3112.

18. Nelson, C.A., Warren, J.T., Wang, M.W., Teitelbaum, S.L., and Fremont, D.H. (2012). RANKL employs distinct binding modes to engage RANK and the osteoprotegerin decoy receptor. Structure *20*, 1971–1982.

19. Baud'huin, M., Duplomb, L., Teletchea, S., Lamoureux, F., Ruiz-Velasco, C., Maillasson, M., Redini, F., Heymann, M.F., and Heymann, D. (2013). Osteoprotegerin: Multiple partners for multiple functions. Cytokine Growth Factor Rev. *24*, 401–409.

20. Malyankar, U.M., Scatena, M., Suchland, K.L., Yun, T.J., Clark, E.A., and Giachelli, C.M. (2000). Osteoprotegerin is an $\alpha_v\beta_3$-induced, NF-κB-dependent survival factor for endothelial cells. J. Biol. Chem. *275*, 20959–20962.

21. Kobayashi-Sakamoto, M., Isogai, E., Hirose, K., and Chiba, I. (2008). Role of α_v integrin in osteoprotegerin-induced endothelial cell migration and proliferation. Microvasc. Res. *76*, 139–144.

22. Mosheimer, B.A., Kaneider, N.C., Feistritzer, C., Djanani, A.M., Sturn, D.H., Patsch, J.R., and Wiedermann, C.J. (2005). Syndecan-1 is involved in osteoprotegerin-induced chemotaxis in human peripheral blood monocytes. J. Clin. Endocrinol. Metab. *90*, 2964–2971.

23. Liu, H., Niu, A., Chen, S.-E., and Li, Y.-P. (2011). β3-integrin mediates satellite cell differentiation in regenerating mouse muscle. FASEB J. *25*, 1914–1921.

24. Ganassi, M., Badodi, S., Wanders, K., Zammit, P.S., and Hughes, S.M. (2020). Myogenin is an essential regulator of adult myofibre growth and muscle stem cell homeostasis. Elife *9*, e60445.

25. Arnold, L., Henry, A., Poron, F., Baba-Amer, Y., van Rooijen, N., Plonquet, A., Gherardi, R.K., and Chazaud, B. (2007). Inflammatory monocytes recruited after skeletal muscle injury switch into antiinflammatory macrophages to support myogenesis. J. Exp. Med. *204*, 1057–1069.

26. Tidball, J.G. (2017). Regulation of muscle growth and regeneration by the immune system. Nat. Rev. Immunol. *17*, 165–178.

27. Hardy, D., Besnard, A., Latil, M., Jouvion, G., Briand, D., Thépenier, C., Pascal, Q., Guguin, A., Gayraud-Morel, B., Cavaillon, J.M., et al. (2016). Comparative study of injury models for studying muscle regeneration in mice. PLoS ONE *11*, e0147198.

28. Ochoa, O., Sun, D., Reyes-Reyna, S.M., Waite, L.L., Michalek, J.E., McManus, L.M., and Shireman, P.K. (2007). Delayed angiogenesis and VEGF production in CCR2−/− mice during impaired skeletal muscle regeneration. Am. J. Physiol. Regul. Integr. Comp. Physiol. *293*, R651–R661.

29. Carlson, B.M., and Faulkner, J.A. (1996). The regeneration of noninnervated muscle grafts and marcaine-treated muscles in young and old rats. J. Gerontol. A Biol. Sci. Med. Sci. *51*, B43–B49.

30. Fielding, R.A., Manfredi, T.J., Ding, W., Fiatarone, M.A., Evans, W.J., and Cannon, J.G. (1993). Acute phase response in exercise. III. Neutrophil and IL-1 β accumulation in skeletal muscle. Am. J. Physiol. *265*, R166–R172.

31. Haydar, D., Cory, T.J., Birket, S.E., Murphy, B.S., Pennypacker, K.R., Sinai, A.P., and Feola, D.J. (2019). Azithromycin polarizes macrophages to an M2 phenotype via inhibition of the STAT1 and NF-κB signaling pathways. J. Immunol. *203*, 1021–1030.

32. Ownby, C.L., Fletcher, J.E., and Colberg, T.R. (1993). Cardiotoxin 1 from cobra (*Naja naja atra*) venom causes necrosis of skeletal muscle in vivo. Toxicon *31*, 697–709.

33. Hawke, T.J., and Garry, D.J. (2001). Myogenic satellite cells: Physiology to molecular biology. J Appl Physiol (1985) *91*, 534–551.

34. Emery, J.G., McDonnell, P., Burke, M.B., Deen, K.C., Lyn, S., Silverman, C., Dul, E., Appelbaum, E.R., Eichman, C., DiPrinzio, R., et al. (1998). Osteoprotegerin is a receptor for the cytotoxic ligand TRAIL. J. Biol. Chem. *273*, 14363–14367.

35. Casar, J.C., Cabello-Verrugio, C., Olguin, H., Aldunate, R., Inestrosa, N.C., and Brandan, E. (2004). Heparan sulfate proteoglycans are increased during skeletal muscle regeneration: Requirement of syndecan-3 for successful fiber formation. J. Cell Sci. *117*, 73–84.

36. Schiaffino, S., Rossi, A.C., Smerdu, V., Leinwand, L.A., and Reggiani, C. (2015). Developmental myosins: expression patterns and functional significance. Skelet. Muscle *5*, 22.

37. Launay, T., Noirez, P., Butler-Browne, G., and Agbulut, O. (2006). Expression of slow myosin heavy chain during muscle regeneration is not always dependent on muscle innervation and calcineurin phosphatase activity. Am. J. Physiol. Regul. Integr. Comp. Physiol. *290*, R1508–R1514.

38. Khaider, N.G., Lane, D., Matte, I., Rancourt, C., and Piché, A. (2012). Targeted ovarian cancer treatment: the TRAILs of resistance. Am. J. Cancer Res. *2*, 75–92.

39. Lane, D., Matte, I., Laplante, C., Garde-Granger, P., Rancourt, C., and Piché, A. (2013). Osteoprotegerin (OPG) activates integrin, focal adhesion kinase (FAK), and Akt signaling in ovarian cancer cells to attenuate TRAIL-induced apoptosis. J. Ovarian Res. *6*, 82.